REVISION - 1

Physio-chemical properties of gamma-irradiated vermiculite and their significance for radiation protection and thermoluminescence

Sukhnandan Kaur*, Surinder Singh, Lakhwant Singh

Department of Physics, Guru Nanak Dev University, Amritsar 143005, Punjab, India

* Corresponding author: sukhnandanphy@gmail.com

Abstract

The present work reports the effects of gamma irradiation of vermiculite for the first time. The radiation induced changes of vermiculite were studied using different techniques viz: ultraviolet-visible spectroscopy (UV-Vis), dielectric measurements, X-ray diffraction (XRD), Fourier Transform Infrared spectroscopy (FTIR) and thermoluminescence (TL). In UV-Vis analysis, the Cody model was employed to calculate structural disorder from Urbach energy which explained the variation of the optical band gap (direct and indirect) with different (1- 2000 kGy) gamma doses. XRD analysis of the pristine and irradiated samples shows that the crystallinity improved upon irradiation at gamma dose upto 1000 kGy and deteriorated on further increase of the gamma dose. A significant change was observed in the dielectric properties after gamma irradiation. Data shows that a.c. conductivity is proportional to the nth power of frequency (f^n) in pristine and irradiated vermiculite, with a slope n ranging between 0.52 and 0.76 which indicates that electronic conduction takes place through an electron hopping process. No appreciable changes in characteristic bands (FTIR) have been observed after irradiation, indicating that natural vermiculite is chemically stable. A well defined TL peak around 132 ^{0}C and enhancement in its intensity with gamma dose (1- 1000 kGy) make vermiculite a perfect thermoluminescence dosimeter and indicates usefulness applications in radiation dosimetry.

Keywords: Natural Vermiculite · Gamma irradiation· Optical properties · Dielectric properties· XRD· FTIR · Thermoluminescence

Introduction

Natural vermiculite is a constituent of the phyllosilicate or sheet silicate group of mineral including Al_2O_3, H_2O, MgO, FeO and SiO_2 which resembles mica in appearance (Brown 1961). Vermiculite is a very important secondary mineral that is formed primarily by the hydrothermal alteration of mica (biotite, phlogopite) or other clay minerals (Basset 1963). Vermiculites are a significant group of clay minerals that consists of two tetrahedral layers as silica and alumina and an octahedral layer of oxygen, magnesium, iron and hydroxyl molecules. Water located between layers is an important part of the vermiculite structure. Vermiculite has long history of applications in insulation, fire resistance, advanced materials, building industry, ceramics, agriculture, horticulture and industrial markets (Strand and Stewart 1983; Hindman 1992; Bergaya et al. 2006; Klein and Dutrow 2007). Nowadays, these natural minerals are in demand due to its high thermal and insulation applications and sensitivity to ionizing radiation. Irradiation of phyllosilicate minerals with gamma and heavy ions leads to remarkable changes in their structural, chemical, optical and electrical properties (Kaur et al. 2013a, 2013b, 2013c).

A significant amount of work has been done on the effect of microwaves on exfoliation properties and thermal behaviour of vermiculite by several groups (Marcos et al. 2009; Muiambo et al. 2010; Marcos and Rodriguez 2011; Folorunso et al. 2013; Campos et al. 2009; Sakharov et al. 2001), but literature survey, on the other hand, revealed no work on gamma irradiated induced modifications of vermiculite. In the present work, effect of gamma irradiation on optical, chemical, structural and dielectric properties of natural vermiculite minerals has been studied for

the first time to identify good materials which have high radiation shielding capacity and thermal insulation property.

Thermo luminescence (TL) is a crucial phenomenon that takes place in various irradiated natural minerals (Kaur et al. 2013c). In order to investigate the thermo luminescent characteristics of vermiculite and to ascertain whether this mineral could qualify as a local dosimeter, the samples of this work were subjected to TL studies. The present research investigates the thermo luminescence response of gamma irradiated natural vermiculite to determine their relevance to dating and radiation dosimetry.

Experimental material and methods

The natural Vermiculite mineral used in the present work was procured from Viozag area in Andhra Pradesh, state of India. The original raw material was cleaved into thin sheets, uniform in thickness and color by using a scalpel. Thickness of each film was measured with a micrometer and is approximately 55±1 μm.

The sheets of vermiculite were further analysed for elemental composition using Energy Dispersive X-ray Spectroscopy (EDS) system attached to a Carl Zesis supra 55 field emission SEM. A thin sheet of vermiculite was placed on a sample holder using silver tape and coated with a layer of gold using a Quorum sputtering coater to make them conductive. Then the sample was transferred to a microscope chamber for EDS measurements. The minimum detectable limit of the EDS system attached with Carl Zesis Supra 55 field emission SEM is 0.2 wt%.

Thin sheets of vermiculite samples of 1 x 1 cm^2 were irradiated at room temperature by γ-radiation using ^{60}Co source from Gamma Chamber-1200 at IUAC, New Delhi to different doses in the range of 1- 2000 kGy. γ-rays emitted by ^{60}Co have a mean energy of 1.25 MeV and the dose rate in the irradiator was 7.5 kGy/h.

The nature of the changes induced by the gamma radiation in vermiculite were examined using HITACHI U-3300 UV-Visible spectrophotometer in the range 200-1100 nm in order to investigate the variation in optical energy gap and Urbach energy. Dielectric properties were analyzed using Hewlett- Packard 4284A LCR meter in the frequency range of 20 Hz- 1 MHz at room temperature. The accuracy of LCR meter for Capacitance- tanδ measurements is 0.05%-0.005% respectively at all text frequencies. The structural studies were carried out by a Bruker AXS X-ray (CuK_{α}, λ =0.154nm) diffractometer for a range of Bragg's angle 2θ ($5<\theta<60$) with scanning speed of 2^0 per minute. FTIR spectra of pristine and irradiated vermiculite were measured by NEXUS-670 FTIR spectrometer, in the range of 4000-400 cm^{-1}. The sheets of vermiculite were crushed and ground in high energy ball mill to prepare the powder samples for TL properties. TL glow curves were recorded at a heating rate of 5 $^0Cs^{-1}$ on a Harshaw TLD reader (Model 3500) taking 5.0 ± 0.2 mg of each sample.

Results and Discussion

EDS Analysis and Optical properties

The EDS analysis indicates that the natural vermiculite mainly consists of silicon (Si), magnesium (Mg), aluminium (Al), iron (Fe) and with some amounts of calcium (Ca) (Table 1). Although the EDS elemental composition analysis are semiquantitative, provided an iron content higher than samples from other sources (Marcos and Rodriguez 2010; Muiambo et al. 2010).

Figure 1 presents the UV-visible absorption spectra of the pristine and gamma irradiated (10, 100, 500, 1000, 1500 and 2000 kGy dose) vermiculite mineral in the wavelength (λ) range 350-1100 nm. A broad absorption band was observed at 704 nm in pristine and gamma irradiated samples which is characteristics of biotite impurity (Karickhoff and Bailey 1973). A shift of absorption edge towards the lower wavelength side was readily observed upto to dose of 1000

kGy, but it shifts towards a much higher wavelength with further increase in dose greater than 1500 kGy (Figure 1). The vermiculite exhibits a blue shift upto gamma dose of 1000 kGy, whereas it exhibit red shift at higher gamma doses upto 2000 kGy. The blue shift shows that the optical band gap of the vermiculite was highly enhanced upto gamma dose of 1000 kGy. Davis and Mott (1979) gave an expression for the absorption coefficient, α ($h\nu$), as a function of photon energy ($h\nu$) for direct and indirect optical transitions through the following equation

$$\alpha (h\nu) = B (h\nu - E_g)^n / h\nu \quad (1)$$

where $h\nu$ is the energy of incident photons, E_g is the value of the optical energy gap between the valence band and the conduction band, B is a constant and the exponent n characterizes the type of electronic transition whether it is a direct or indirect band transition. Specifically, n is 1/2 and 2 for direct and indirect optical band gap respectively. The $(\alpha h\nu)^{1/2}$ and $(\alpha h\nu)^2$ were plotted as a function of photon energy ($h\nu$) respectively, to determine indirect and direct band gap. The calculated optical energy band gaps E_g (direct and indirect) of the pristine and gamma irradiated samples tabulated in Table 2. The direct and indirect energy band gap in vermiculite has been observed for the first time as no such report was found in literature survey. The value of the optical direct and indirect band gap increases with the increase in gamma dose upto 1000 kGy, however decreases with further increase in gamma dose upto 2000 kGy (Table 2).

Urbach energy (E_u) is another parameter which gets significantly affected by irradiation. The irregularities in the band gap level can be defined in terms of Urbach energy. It depends on induced disorder, static disorder, temperature and thermal vibrations in the lattice and on average photon energies. The Urbach energy is estimated using relation (Urbach 1953)

$$\alpha(\nu) = \alpha_o \exp(h\nu/E_u) \quad (2)$$

where hν is the photon energy, α_o is a constant, E_u is the Urbach's energy and $\alpha(\nu)$ is an absorption coefficient. The logarithm of the absorption coefficient $\alpha(\nu)$ as a function of the photon energy (hν) for the pristine and gamma irradiated samples is plotted and Urbach energy can be calculated by taking the slope of the linear part of the plot. The calculated values are listed in Table 2.

Cody et al. (1981) first established the relationship between the structural disorder, the Urbach's energy and the temperature (T) for explaining the optical absorption characteristics and has the form

$$E_u = \frac{E_p}{2\sigma_0}\left[X + \coth\left(\frac{E_p}{2k_BT}\right)\right] \quad (3)$$

where E_p is the phonon energy, σ_0 is Urbach edge parameter of order unity, k_B is Boltzmann constant and X is a measure of structural disorder which is defined as the ratio of the mean square deviation of atomic position $\langle U^2 \rangle$ to the zero-point uncertainty in the atomic position squared $\langle U_0^2 \rangle$

$$X = \frac{\langle U^2 \rangle}{\langle U_0^2 \rangle} \quad (4)$$

An average value of phonon energy in natural vermiculite is 73.7 meV, as determined by Raman spectroscopy (Rakhshani, 2000). The structural disorder parameter 'X' for each Urbach energy value at temperature of 22 °C is calculated using equation (3) and given in Table 2. The decrease of the Urbach energy with increase in gamma dose upto 1000 kGy indicates the decrease in the structural disorder (Table 2). By further increasing the gamma dose upto 2000 kGy, the increase in the Urbach energy may be attributed to increase in the structural disorder.

The Urbach energy decreases with increase of gamma dose upto 1000 kGy (Table 2), which may be due to the decrease of structural disorder (X), which in turns leads to increases the optical band gaps (direct and indirect). The observed increase in the optical band gap and decrease in the Urbach energy both arise due to decrease in structural disorder of vermiculite. However, with further increase in gamma dose upto 2000 kGy the Urbach energy increases abruptly due to a remarkable increase in the structural disorder. This means that the higher gamma dose produces defects, dislocations and disorder in the vermiculite structure, which in turn leads to decrease the optical band gaps (direct and indirect).

Dielectric Properties

The capacitance and tanδ (loss factor) of the vermiculite were measured for varying frequencies from 20 Hz to 1 MHz at room temperature. Two probe method involves sandwiching a thin sheet of vermiculite between the two electrodes to form a capacitor (Kaur et al. 2013 c).The dielectric constant (ε') and the dielectric loss (ε'') of the vermiculite were calculated by using the relations:

$$\varepsilon' = \frac{Cd}{A\varepsilon_o} \quad (5)$$

$$\varepsilon'' = \varepsilon' \tan\delta \quad (6)$$

where C is capacitance (F), d is the thickness (m), ε_o is the free space permittivity (ε_o = 8.854 x 10^{-12} F/m) and A the area of the sample (m^2). The ac electrical conductivity (σ_{ac}) of the dielectric material is given by the following equation:

$$\sigma_{ac} = \varepsilon'\varepsilon_o\omega\tan\delta \quad (7)$$

where $\omega = 2\pi f$ is the angular frequency. The electric modulus (M^*) is defined as

$$M^* = M' + iM'' \quad (8)$$

156 The real (M') and imaginary (M'') parts of electric modulus (M^*) can be calculated by using the
157 following relation:

158 $$M' = \frac{\varepsilon'}{(\varepsilon')^2 + (\varepsilon'')^2} \quad (9)$$

159 $$M'' = \frac{\varepsilon''}{(\varepsilon')^2 + (\varepsilon'')^2} \quad (10)$$

160 The calculated values of dielectric parameters using the above relations (5-10) are listed in Table
161 3 for different gamma doses at constant frequency of 400 kHz. The dielectric constant decreases
162 with increase of frequency (Figure 2). The dielectric constant is high in the low frequency region
163 and decreases continuously with increase in frequency before and after irradiation. The high
164 value of dielectric constant in the lower frequency region can be assigned to the presence of
165 interfacial i.e., space charge polarization mechanism and ionic conduction. The reduction of the
166 value of dielectric constant at higher frequencies may be due to the loss of significance of these
167 polarizations gradually. Figure 2 also shows that the dielectric constant increases with increasing
168 gamma dose up to 1000 kGy, however it decreases with further increase of gamma dose upto
169 2000 kGy. The loss factor (tanδ) versus frequency plots for pristine and gamma irradiated
170 vermiculite show positive values that indicate the inductive dominance (Figure 3). The low loss
171 tangent is observed in the gamma dose range of 10- 1000 kGy which concludes that the
172 vermiculite irradiated in this range possesses good optical quality and defect number is very low.
173 The dielectric loss shows the same behaviour as that of tanδ with increase of gamma dose
174 (Figure 4). The values of ε'', tanδ, σ_{ac}, M' and M'' are all lower in the dose range 10- 1000
175 kGy (Table 3). However, these dielectric parameters show an increase with further increase in
176 gamma dose upto 2000 kGy. The reduction of dielectric parameters at gamma dose of 10- 1000
177 kGy may be assigned to the healing effects of radiation, however irradiation induced defect (see

above- optical properties) becomes more prominent at higher gamma doses of 2000 kGy which in turn raises the values of these parameters. This means that there is coexistence for the creation and annihilation of defects at gamma doses upto 1000 kGy; at higher gamma doses (2000 kGy), the number of defects induced by irradiation becomes larger than the number of defects annihilated.

The complex impedance Z^* of the present material can be described by the following equation:

$$Z^* = Z' - iZ'' \quad (11)$$

where Z' and Z'' are ascribed to real and imaginary parts of impedance. The relation between electric modulus and complex impedance is given by:

$$M^* = i\omega C_0 Z^* \quad (12)$$

In the above equations ω is the angular frequency (=2πf), C_0 is the vacuum capacitance of the measuring cell and electrodes with an air gap of the dimensions of the sample thickness.

$$C_0 = \frac{\varepsilon_0 A}{d} \quad (13)$$

where ε_o is the free space permittivity, d is the thickness and A the area of the sample. The values of Z' and Z'' calculated by substituting the values of M^* and Z^* from equations (9) and (11) in to equation (12) and are as follow:

$$Z' = \frac{\omega C_0}{M''} \quad (14)$$

$$Z'' = \frac{\omega C_0}{M'} \quad (15)$$

The calculated values of Z' and Z'' from above relation for different gamma dose are enlisted in Table 3. It is observed that the values of Z' and Z'' increases with increase in gamma dose upto 1000 kGy, which means the gamma dose enhances its insulation properties upto this gamma

dose (Table 3). These results also support the enhancement in dielectric constant with gamma dose. However, with further increase of gamma dose upto 2000 kGy, the values of Z' and Z'' decreases which indicates the reduction of dielectric constant.

A convenient formalism to investigate the frequency dependence of ac conductivity in a material is based on the power law relation proposed by Jonscher (1996)

$$\sigma_{ac} \propto f^n \quad (16)$$

where the frequency exponent n is temperature independent. The frequency dependence of the ac conductivity of pristine and gamma irradiated vermiculite samples are shown in Figure 5 and the values of n have been calculated from the slope of these straight lines. The calculated values of n lies between 0.52 to 0.76. These are less than unity and together with the linear dependence of ac conductivity indicates that the electrical conductivity may be ruled by an electron hopping process. The similar result was observed previously in other minerals (Kaur et al. 2013b, 2013c).

Structural Analysis

Figure 6 shows the XRD pattern for vermiculite in pristine and irradiated up to the gamma dose of 2000 kGy. In pristine vermiculite five peaks are observed at $2\theta = 8.87^0$, 26.67^0, 35.79^0, 45.14^0 and 54.83^0. These peaks do not show any change in their positions on irradiation with different gamma doses. This indicates that there is no change in the basic crystalline structure of vermiculite. The peaks become sharper and intensity of these peaks also increases with increasing of gamma dose upto 1000 kGy, indicating the enhancement of crystallinity and ordering in the vermiculite. However, with further increase in gamma dose upto 2000 kGy the peaks become broader (Table 4) and intensity decreases which denotes some destruction of the orderliness of the original crystal. The mean crystallite size (D), micro strain (S) and dislocation density (δ) have been be estimated using Williamson-Hall (W-H) analysis from the XRD. W-H

222 analysis is a simplified integral breadth method where both size-induced and strain-induced
223 broadening is deconvoluted by considering the peak width as a function of 2θ (Williamson and
224 Hall 1953). The crystallite size (D) was calculated using Debye Scherrer formula from the full
225 width half maximum (FWHM) measurements

226 $$D = \frac{K\lambda}{\beta \cos\theta} \quad (17)$$

227 here, K is a constant which depends on diffractometer setup, λ is wavelength of X-ray, θ is
228 diffraction angle or Bragg's angle and β denotes FWHM. In the present setup K = 0.9 and λ =
229 1.541 Å. The values of β and θ can be obtained from the diffraction pattern (Figure 6).The
230 microstrain (S) arising from crystal imperfection and distortion was calculated using formula

231 $$S = \frac{\beta}{4\tan\theta} \quad (18)$$

232 The observed line width is simply the sum of equations (17) and (18)

233 $$\beta = \frac{\lambda}{D\cos\theta} + 4S\tan\theta \quad (19)$$

234 By rearranging the above equation,

235 $$\frac{\beta\cos\theta}{\lambda} = \frac{1}{D} + S\left(\frac{4\sin\theta}{\lambda}\right) \quad (20)$$

236 The above equation is known as Williamson-Hall equation. The plot of $\left(\frac{\beta\cos\theta}{\lambda}\right)$ versus
237 $\left(\frac{4\sin\theta}{\lambda}\right)$ gives the value of the microstrain from slope and the crystallite size from the ordinate
238 intercept. Figure 7 shows the W-H plots for the pristine and the gamma irradiated vermiculite at
239 different gamma doses. The values of crystallite size (D) and microstrain (S) obtained from the
240 intercept and slope of W-H plots are listed in Table 4. A negative slope in the W-H plot indicates

241 the presence of compressive strain experienced by the particle of vermiculite. The dislocation
242 density (δ) calculated using the following formula (Kulg and Alexander 1974) is listed in Table
243 4:

244 $$\delta = \frac{15S}{aD} \quad (21)$$

245 A significant enhancement in crystallite size in irradiated vermiculite samples is observed upto to
246 gamma dose of 1000 kGy; micro strain (S) and dislocation density (δ) decreases in the gamma
247 dose range of 10- 1000 kGy (Table 4). With further increase in gamma dose upto 2000 kGy, the
248 crystallite size decreases, however, unlike the microstrain and dislocation density which increase.
249 This increase in crystallite size in the dose 10- 1000 kGy is due to the formation of some large
250 size crystallites due to irradiation. This binding of small crystallites increases the crystallite size
251 and decreases the micro strain in the structure which in turn decreases the dislocation density
252 (Table 4). This means that increased ordering of vermiculite structure takes place in the gamma
253 dose range 10- 1000 kGy. This is attributed to the improvement in the crystallinity due to the
254 increase in crystallite size, reduction in the defects and the decrease in structural disorder and
255 microstrain. A higher gamma doses upto 2000 kGy, the crystallite size decreases and micro
256 strain and dislocation density increases which indicate convergence of the vermiculite towards a
257 more disordered system. These results are in good agreement with the UV-Vis and dielectric
258 results.

259 **FTIR Analysis**

260 The FTIR spectrum of the pristine and gamma irradiated natural vermiculite illustrates the
261 characteristics bands of natural vermiculite (Muiambo et al. 2010) (Figure 8). A strong
262 absorption band is observed corresponding to the stretching vibration of the Mg_3-OH groups
263 located at 3443 cm^{-1} related to OH hydroxyl groups of interlamellar water in the pristine

vermiculite sample. The infrared band observed at 2350 cm^{-1} revealed the presence of chemisorbed CO_2. The absorption band appearing at 1642 cm^{-1} is attributed to O–H bending vibrations of the hydration water molecules. A strong band observed at 1004 cm^{-1} is assigned to Si–O–Si and Si–O–Al stretching vibrations. The band appearing at 682 cm^{-1} is associated with Si–O deformation. No new band has been observed in irradiated samples. Hence, gamma irradiation did not induce any significant changes in the bonds, however, the changes in the overall intensity of the transmittance after irradiation was observed (Figure 8). The intensity of the transmittance increases with increase of gamma dose upto 1000 kGy. With further increase of gamma dose upto 2000 kGy, the intensity decreases which indicate structural deformation of vermiculite after irradiation (Kaur et al. 2013c). This agrees well with the results of UV-VIS absorption spectra and XRD as discussed earlier.

Thermoluminescence Analysis

The TL glow curves of vermiculite exposed to gamma radiation at different doses (1- 2000 kGy) are depicted in Figure 9. A glow curve of the vermiculite irradiated at different gamma doses consists of one prominent peak around 132 ^{0}C, known as a dosimetry peak. The glow curves obtained at all gamma doses show almost the same shape and peak position (Figure 9). The TL intensity of the glow peak enhances systematically with the increase of gamma dose, which indicates that this peak is a radiation sensitive peak. Increase in intensity of glow peaks by gamma irradiation may be due to the increase in the number of traps into the lattice. It is also noticed that though the TL intensity of 132 ^{0}C glow peak of vermiculite increases with increase in gamma dose but there is no appreciable shift in peak temperature.

The TL response curve of vermiculite irradiated by various gamma doses is exhibited in Figure 10 in which the height of 132 ^{0}C main TL glow peak was used for measuring the TL intensity

and the error bars indicates the standard deviation of three measurements from their average value. The TL dose response curve shows almost linear behavior in the dose range of 1 kGy to 1000 kGy. This linear behavior over a wide range of gamma dose (1- 1000 kGy) may be due to the fact that number of electrons in the excited state increases with increase of the gamma dose and hence there is a possibility of increase of recombination as well as TL emission. After a gamma exposure of 1500 kGy, a decrease in TL intensity has been noticed with further increase in dose. This fall in the TL intensity at higher doses might be due to the damage of the TL trap. The activation energy of the trap depth (E) calculated using the empirical formulae (El-Kolaly et al. 1994):

$$E(eV) = \frac{T_P(K)}{464} \qquad (22)$$

where T_P is the peak temperature of the TL glow curve. Since the position of the obtained glow peaks is more or less independent of gamma dose, therefore the values of the activation energy of all the trap depths are same and was found to be E = 0.87 eV. Thus a distinct radiation sensitive glow peak and linear dose response upto wide range (1- 1000 kGy) leads us to conclude for the first time that natural vermiculite is a suitable material for TL dosimeter in radiation rich environment.

Implications

In the present work, effect of gamma irradiation on optical, chemical, structural and dielectric properties of natural vermiculite minerals have been studied for the first time and indicates that vermiculite is a material that has high radiation shielding capacity and thermal insulation properties. The enhancement in opto-electric properties of vermiculite with gamma irradiation also makes it suitable for optoelectronic devices. Gamma irradiation did not induce any significant changes in the bonds, hence vermiculite is chemically stable. Thermoluminescence

properties demonstrate the applicability of natural vermiculite as a cost effective TL dosimeter for innovational dosimetry in radiation rich environs.

Conclusions

The results of opto-structural, dielectric, chemical and thermoluminescence properties of γ-irradiated vermiculite indicates that irradiation induces structural changes that lead to the creation of new material with the enhanced properties. It is concluded from UV-Vis analysis that the increase of optical band gap with gamma irradiation makes natural vermiculite mineral a good candidate for efficient optoelectronic devices. A notable increase in the dielectric constant of the vermiculite with gamma dose of 1000 kGy has been observed which improves its utility as an electronic insulator. A negative slope in the Williamson-Hall plot indicates the presence of compressive strain experienced by the particle of vermiculite. Gamma irradiation upto 1000 kGy leads to the improvement in the crystallinity due to the increase in crystallite size, reduction in the defects and the decrease in structural disorder and microstrain. The results at higher doses reveal that the microstrain and dislocation density increases which leads to the production of defects and structural disorder. The outcomes of FTIR analysis are in good agreement with the UV-Vis, Dielectric and XRD results. From the TL studies, it is confirmed that natural vermiculite is a good material for TL dosimeter for innovative dosimetry applications in radiation rich environment. Thus we can conclude that the gamma irradiation can be utilized as a tool for tailoring the various properties of vermiculite in the field of insulation and radiation rich environment.

Acknowledgements

Authors are highly thankful to Health physics and material science group at IUAC, New Delhi for providing the gamma irradiation, TL, dielectric measurements, and FTIR facilities. Financial

support given by UGC, New Delhi, in the form Senior Research Fellowship is also gratefully acknowledged.

References

Basset,W.A. (1963)The geology of vermiculite occurrences. Clays and Clay Minerals, 10, 61-96.

Bergaya, F., Theng, B.K.G., and Lagaly, G. (2006) Handbook of Clay Science. Elsevier.

Brown, B. (1961) The X-Ray identification and crystal structures of clay minerals. Mineralogical Society, London.

Campos, A., Moreno, S., and Molina, R. (2009) Characterization of Vermiculite by XRD and spectroscopic techniques. Earth Sciences Research Journal, 13, 108-118.

Cody, G.D., Tiedje, T., Abeles, B., Brooks, B., and Goldstein, Y. (1981) Disorder and the Optical-Absorption Edge of Hydrogenated Amorphous Silicon. Physical Review Letters. 47, 1480- 1483.

El-Kolaly, M.A., Kassema, M.E., Higazy, A., Ismaila, L.Z., and Alhouty, L.I. (1994) Thermoluminescence and dielectric response of $LiKSO_4$: Gd to γ-radiation. Radation Physics and Chemistry, 44, 441-446.

Folorunso, O., Dodds, C., Dimitrakis, G., and Kingman, S. (2012) Continuous energy efficient exfoliation of vermiculite through microwave heating. International Journal of Mineral Processing, 114-117, 69-79.

Hindman, J.R. (1992) Vermiculite, Vermiculite Technology, News Letter, 3A, 12p.

Jonscher, A.K. (1996) Universal Relaxation Law. Chelsea Dielectric Press, London.

Karickhoff, S.W. and Bailey, G.W. (1973) Optical absorption spectra of clay minerals. Clays and Clay Minerals, 21, 59-70.

Kaur, S., Singh, S., Singh, L., and Lochab, S.P. (2013a) Oxygen ion-induced modifications of optical properties of natural muscovite mica. Radiation Effects and Defects in Solids, 168, 587-593.

Kaur, S., Singh, S., Singh, L., and Lochab, S.P. (2013b) Effect of Gamma irradiation on Opto-structural, Dielectric and Thermoluminescence properties of Natural Phlogopite Mica. Journal of Applied Physics, 114, 093503, 1-7.

Kaur, S., Singh, S., Singh, L., and Lochab, S.P. (2013c) Opto-structural and dielectric properties of 80 MeV oxygen ion irradiated natural phlogopite mica. Nuclear Instruments and Methods in Physics Research B, 301, 17-22.

Klein, C. and Dutrow, B. (2007) Manual of Mineral Science, 23p. Wiley, New York.

Kulg, H.P. and Alexander, L.E. (1974) X-Ray diffraction procedures. Wiley, New York.

Marcos, C., Arango, Y.C., and Rodriguez, I. (2009) X-ray diffraction studies of the thermal behaviour of commercial vermiculites. Applied Clay Science, 42, 368-378.

Marcos, C., and Rodriguez, I. (2010) Expansion behaviour of commercial vermiculites at 1000 ^{0}C. Applied Clay Science, 48, 492- 498.

Marcos, C., and Rodriguez, I. (2011) Expansibility of vermiculites irradiated with microwaves. Applied Clay Science, 51, 33-37.

Mott, N.F. and Davies, E.A. (1979) Electronic Processes in Non- crystalline materials. Claredon Press, Oxford.

Muiambo, H.F., Focke, W.W., Atanasova, M., Westhuizen, I. van der., and Tiedt, L.R. (2010) Thermal properties of sodium-exchanged palabora vermiculite. Applied Clay Science, 50, 51-57.

Rakhshani, A.E. (2000). Study of Urbach tail, bandgap energy and grain-boundary characteristics in CdS by modulated photocurrent spectroscopy. Journal of Physics: Condensed Matter, 12, 4391- 4400.

Sakharov, B.A., Dubinska, E., Bylina, P., and Kapron, G. (2001) Unusual X-ray characteristics of vermiculite from Wiry, Lower Silesia, Poland. Clays and Clay Minerals, 49, 197-203.

Strand, P.R., and Stewart, E. (1983) Industrial Mineral and Rocks. The Society of Mining Engineers of the American Institute of Mining, Metallurgical and Petroleum Engineers, New York, pp. 1375–1381.

Urbach, F. (1953) The Long-Wavelength Edge of Photographic Sensitivity and of the Electronic Absorption of Solids. Phys. Rev. 92, 1324.

Williamson, G.K., Hall, W.H., 1953. X-ray line broadening from filed Aluminium and Wolfram. Acta Metallurgica, 1, 22-31.

Figure Captions

Figure 1. UV-Vis spectra of pristine and gamma irradiated vermiculite.

Figure 2. Dielectric constant (ε') versus frequency for pristine and gamma irradiated vermiculite.

Figure 3. Tanδ versus frequency for pristine and gamma irradiated vermiculite.

Figure 4. Dielectric loss (ε'') versus frequency of pristine and gamma vermiculite.

Figure 5. Frequency dependence of ac conductivity for pristine and gamma irradiated vermiculite.

Figure 6. X- ray diffraction pattern for pristine and gamma irradiated vermiculite.

Figure 7. Williamson Hall plots for the pristine and gamma irradiated vermiculite.

Figure 8. FTIR spectra of pristine and gamma irradiated vermiculite.

Figure 9. TL glow curves of vermiculite irradiated with gamma rays at different doses.

Figure 10. TL glow peak intensity vs gamma dose for vermiculite.

424 **Table 1.** EDS elemental composition analysis of natural vermiculite

425

Element	Weight%	Atomic%
Si	24.45	19.03
Al	10.69	8.67
Mg	10.19	9.16
Fe	10.51	4.12
Ca	1.61	0.88
O	42.55	58.15
Total	100.00	100.00

426

427

428 **Table 2.** The variation of optical band gap energy, Urbach's energy and structural disorder with
429 gamma dose in the pristine and gamma irradiated vermiculite

Gamma Dose (kGy)	*Band Gap Energy (eV)		*Urbach 's energy (eV)	Structural Disorder (X)
	Indirect	Direct		
Pristine	1.04	2.02	1.28	33.57
10	1.19	2.23	1.24	32.48
100	1.32	2.33	1.18	30.86
500	1.58	2.57	1.04	27.06
1000	1.68	2.71	0.98	25.44
1500	0.78	1.83	1.32	34.65
2000	0.71	1.78	1.35	35.46

430 *Standard deviation is ±0.01

431

432

433

434 **Table 3.** The variation of dielectric parameters with gamma dose in the pristine and Gamma
435 irradiated vermiculite.

Gamma Dose (kGy)	ε'	ε''	Tanδ (1×10^{-1})	σ_{ac} (1×10^{-10}) ($\Omega^{-1}m^{-1}$)	M' (1×10^{-1})	M'' (1×10^{-4})	Z' (Ω) (1×10^{-3})	Z'' (Ω) (1×10^{-5})
Pristine	21.96	0.44	0.20	9.78	0.46	9.11	2.92	2.72
10	22.04	0.38	0.17	8.48	0.45	7.85	3.50	2.77
100	22.90	0.34	0.15	7.58	0.44	6.49	6.05	2.86
500	24.05	0.20	0.08	4.49	0.42	3.49	13.89	3.00
1000	24.72	0.13	0.05	2.94	0.40	2.17	60.39	3.11
1500	23.69	0.27	0.11	5.93	0.42	4.75	8.54	2.94
2000	22.25	0.37	0.17	8.30	0.45	7.54	4.46	2.79

436

437

438 **Table 4.** Results of Williamson –Hall plots

Gamma Dose (kGy)	Peak Width (β) (10^{-2}) ($2\theta = 8.87^0$)	*Average Domain Size (D) nm	Microstrain (S) (10^{-4})	Dislocation Density (δ) (10^{-5})
Pristine	13.942	63.25	7.79	3.48
10	9.768	72.88	6.10	2.36
100	7.632	88.96	3.40	1.08
500	6.008	109.05	2.37	0.61
1000	5.011	132.62	1.79	0.38
1500	7.034	75.99	3.19	1.18
2000	10.288	55.58	8.77	4.46

439 *Standard deviation is ±0.05

440

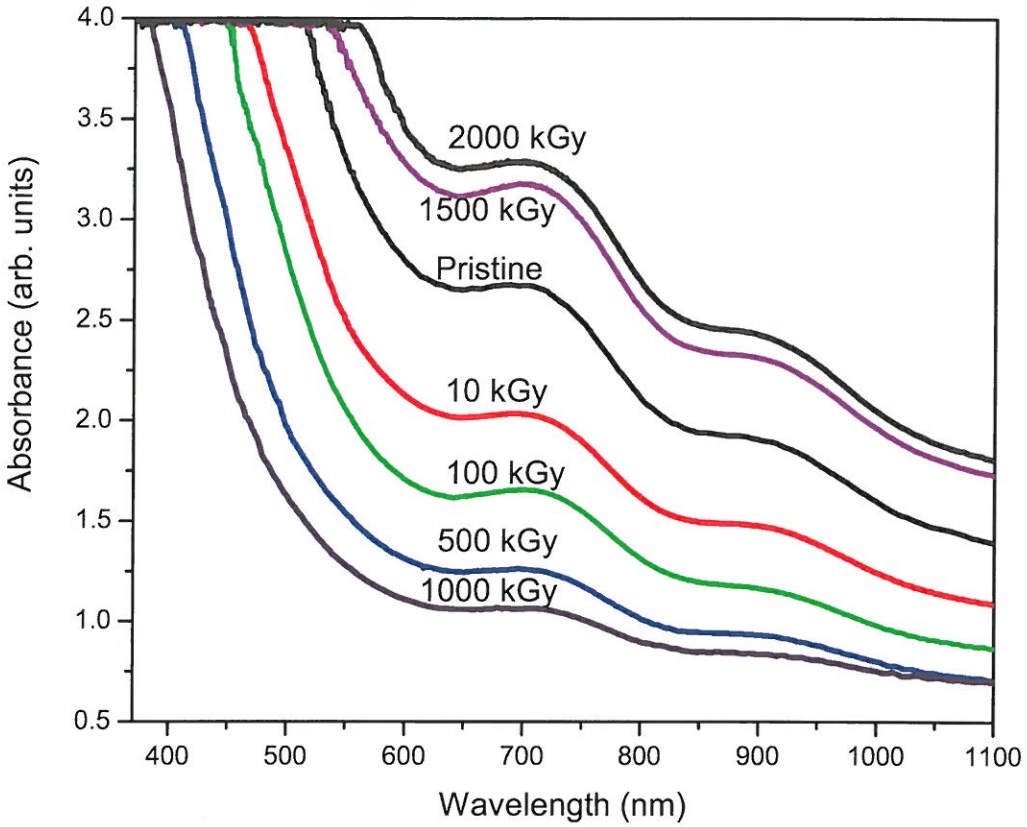

441

442 **Figure 1.** UV-Vis spectra of pristine and gamma irradiated vermiculite.

443

444

445

446

447

448

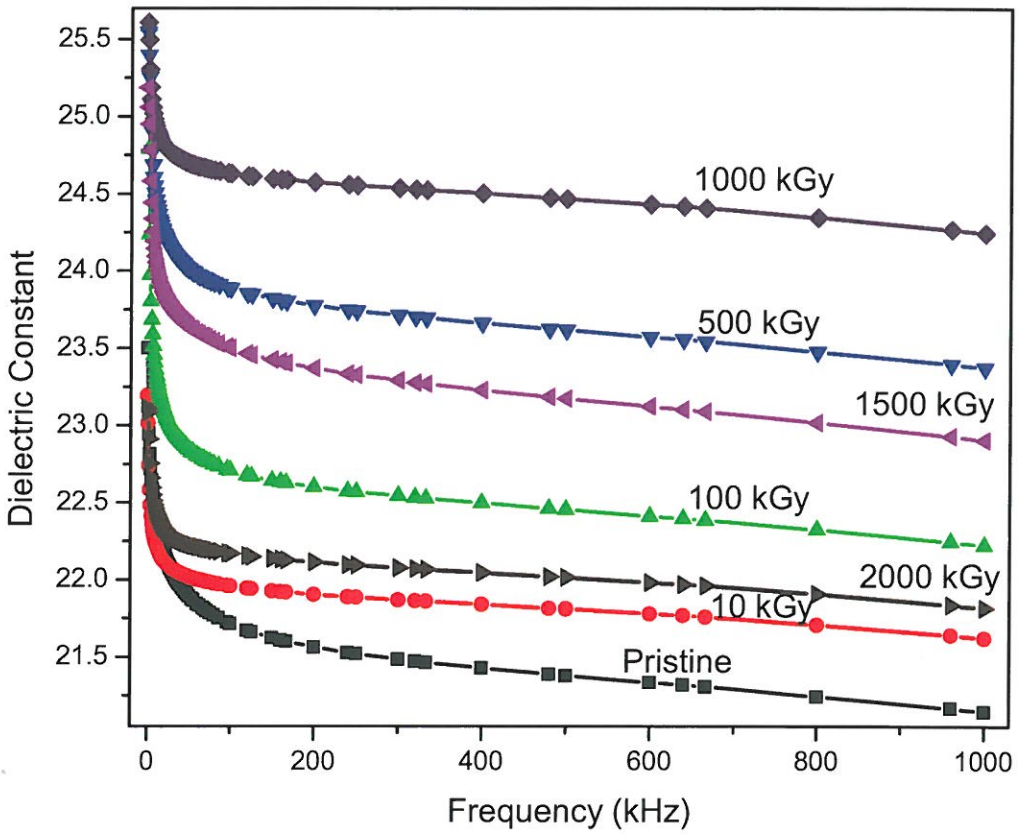

449

450 **Figure 2.** Dielectric constant (ε') versus frequency for pristine and gamma irradiated
451 vermiculite.

452

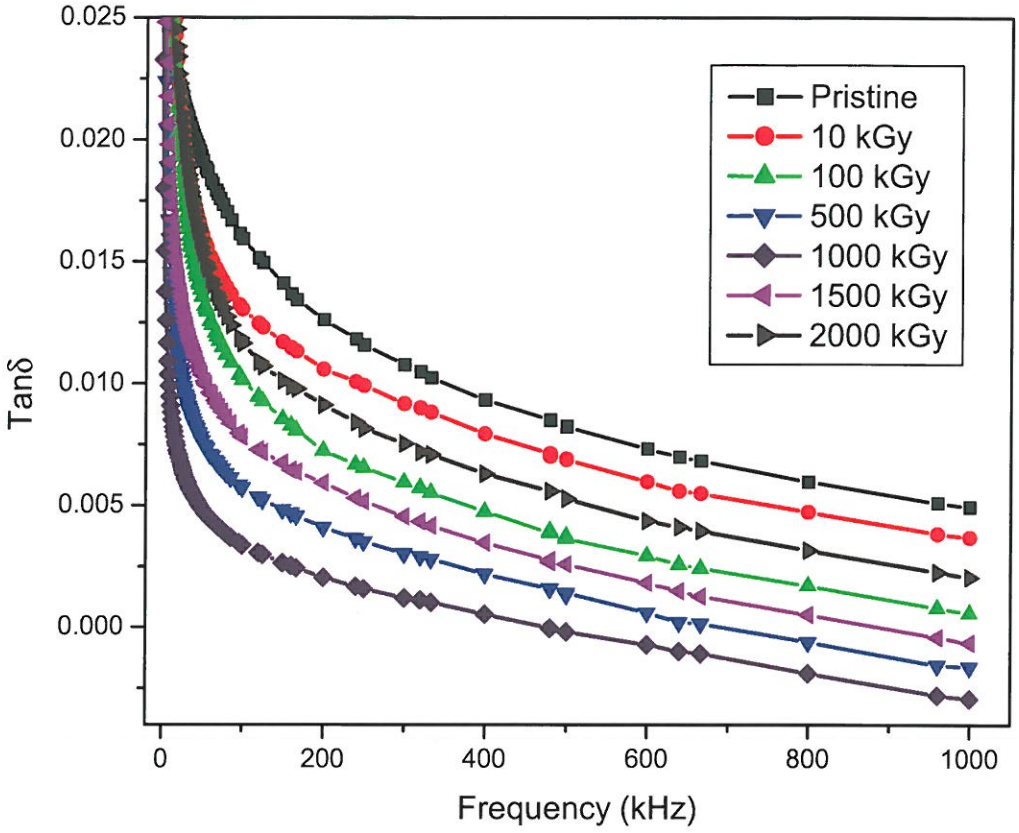

453

454 **Figure 3.** Tanδ versus frequency for pristine and gamma irradiated vermiculite.

455

456

457

458

459

460

461

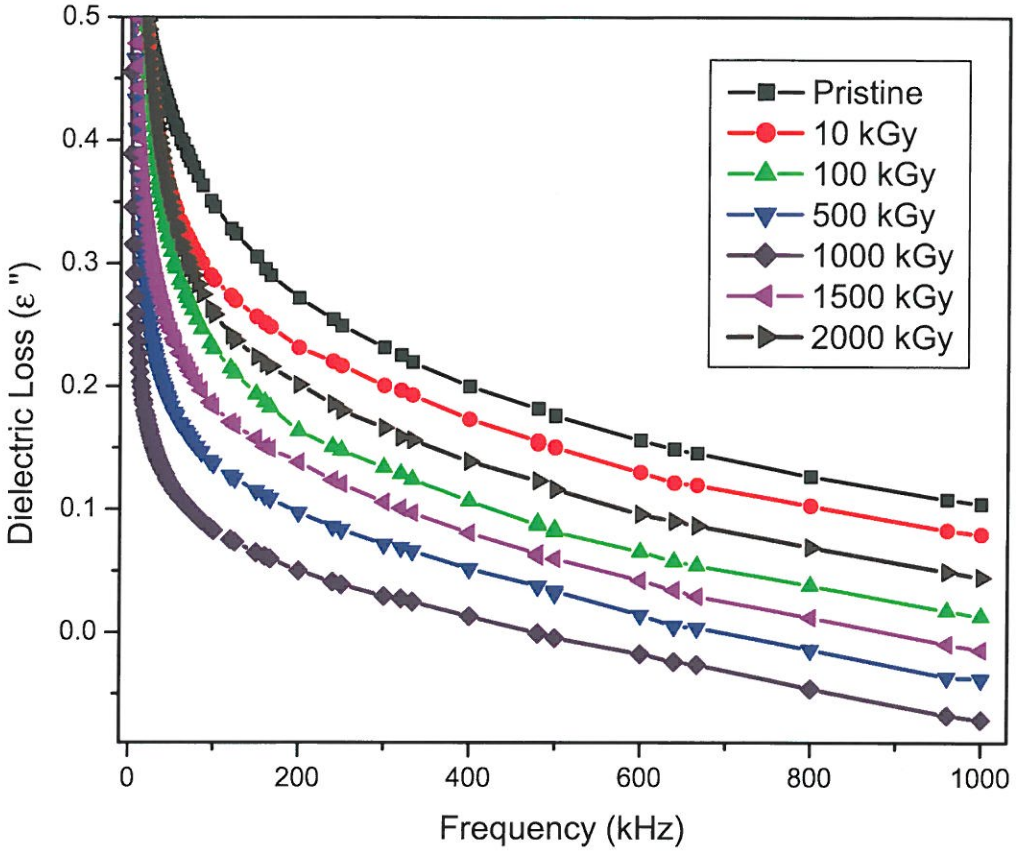

462

463 **Figure 4.** Dielectric loss (ε'') versus frequency of pristine and gamma vermiculite.

464

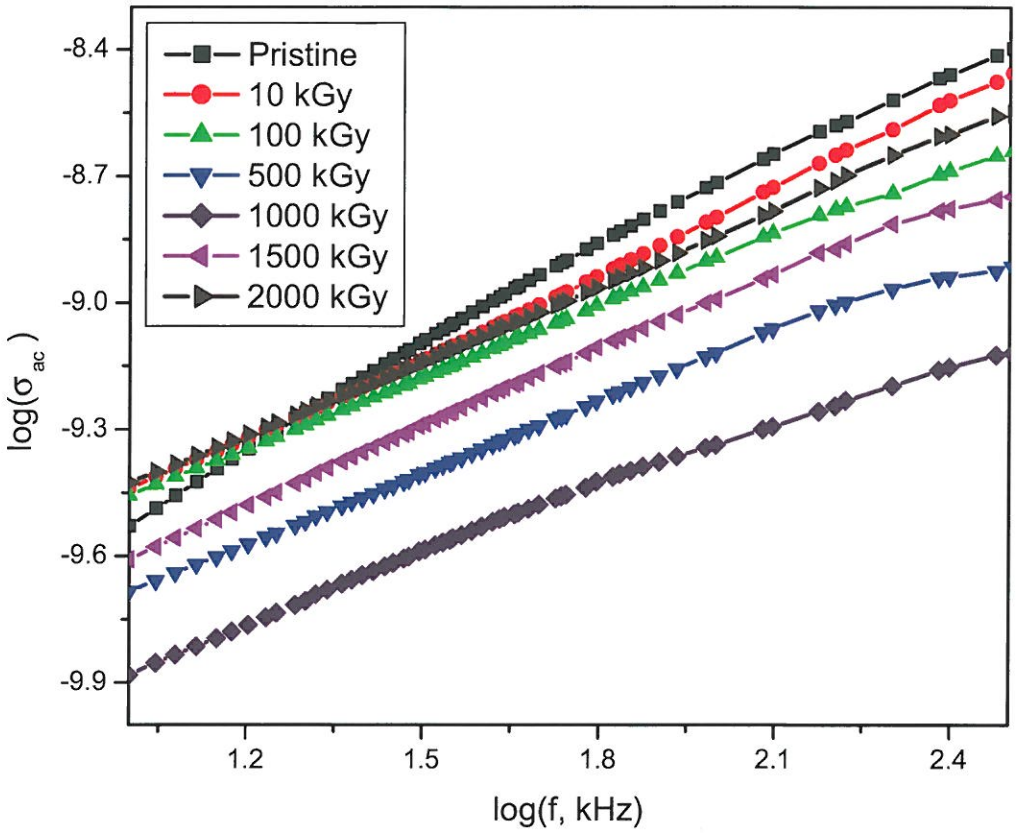

Figure 5. Frequency dependence of ac conductivity for pristine and gamma irradiated vermiculite.

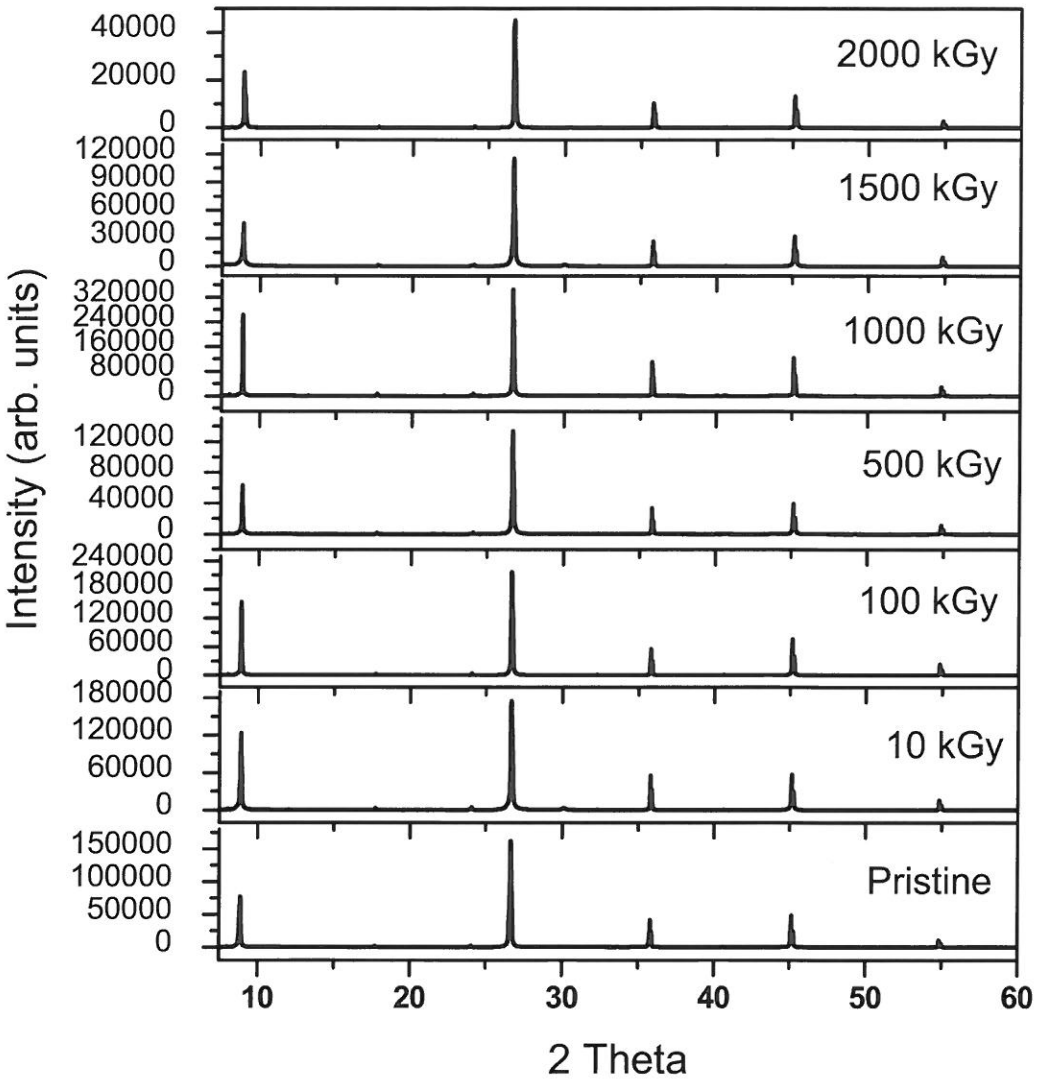

Figure 6a. X- ray diffraction pattern for pristine and gamma irradiated vermiculite.

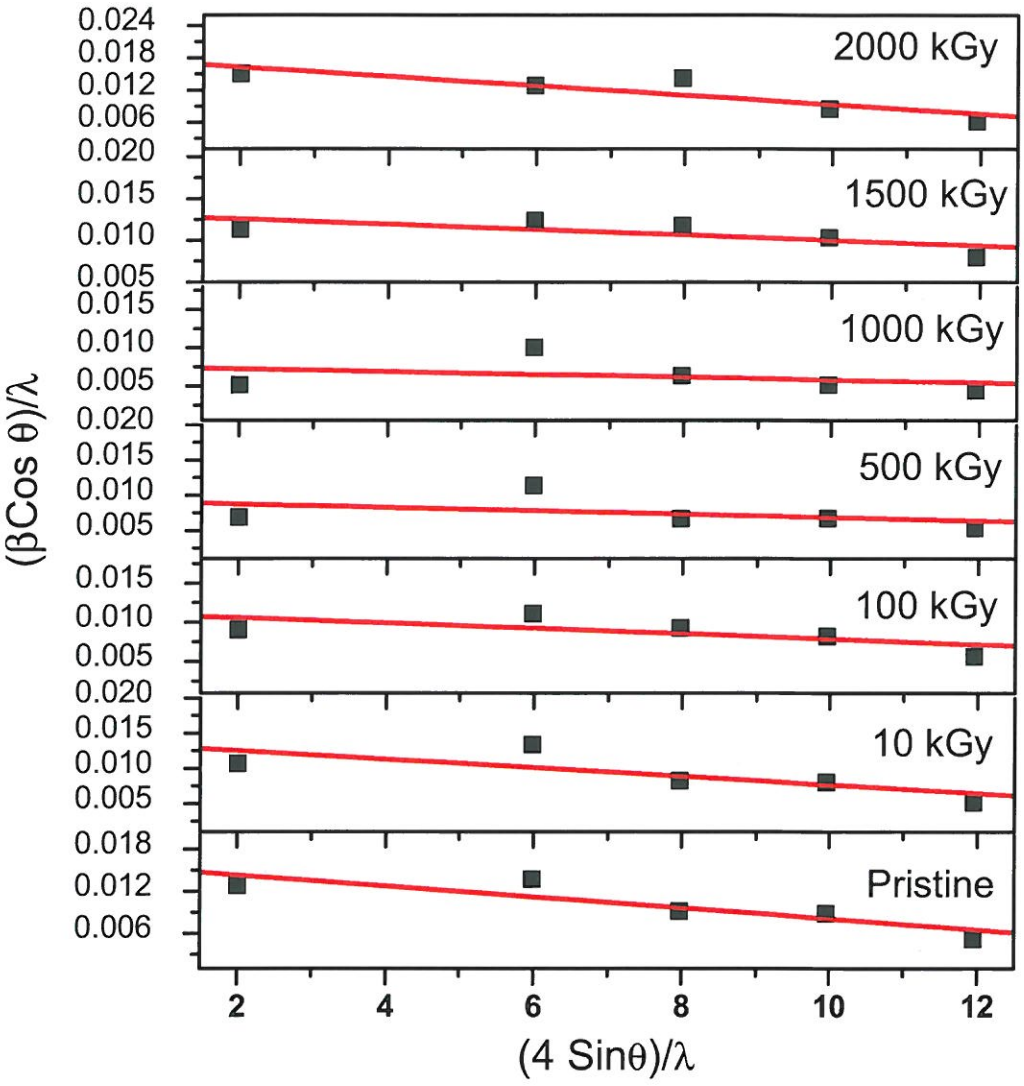

Figure 7. Williamson Hall plots for the pristine and gamma irradiated vermiculite.

487

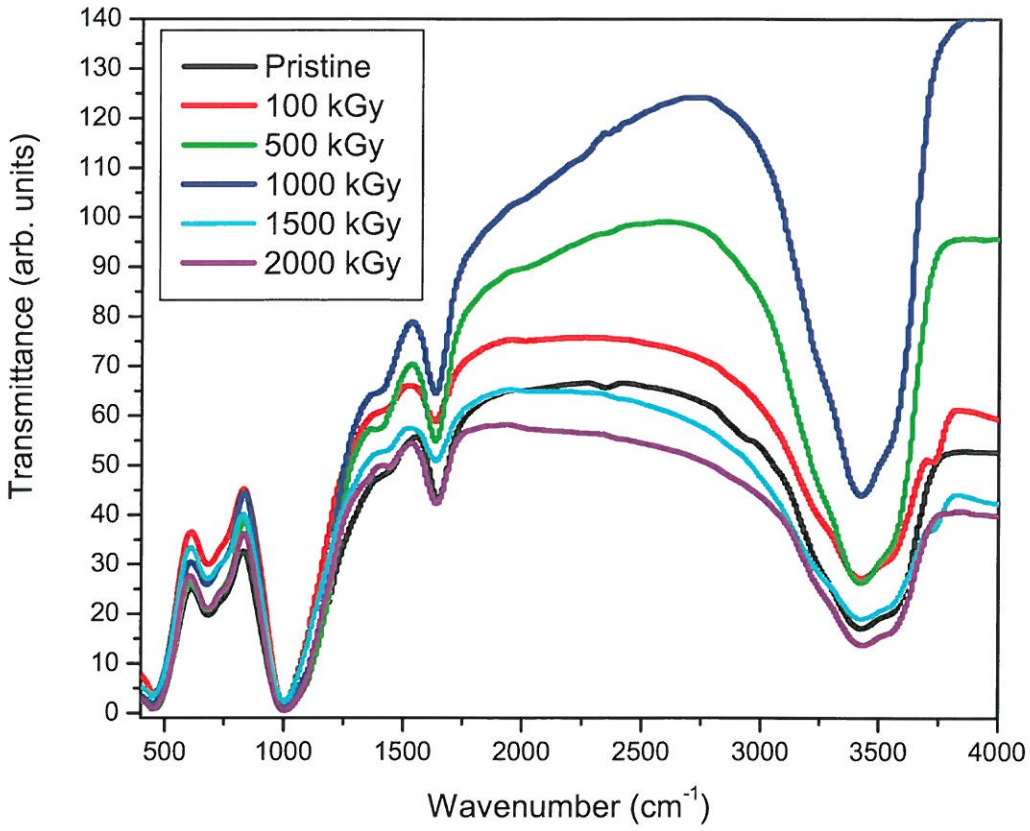

488

489 **Figure 8.** FTIR spectra of pristine and gamma irradiated vermiculite.

490

491

492

493

494

495

496

497

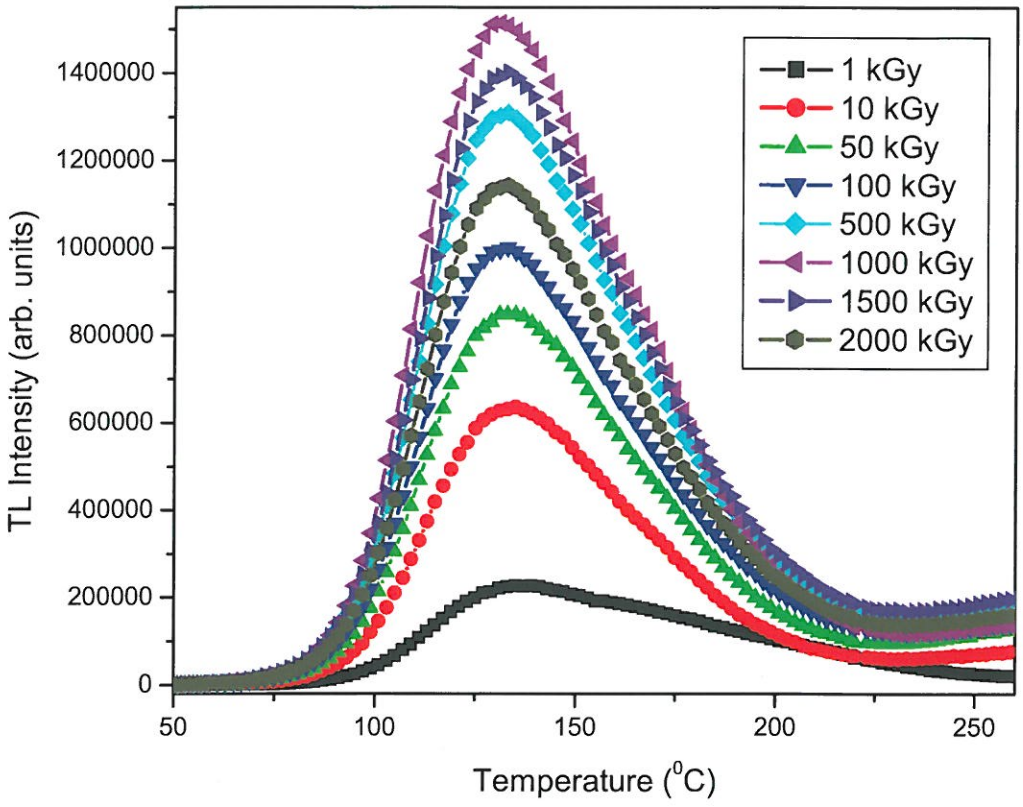

498

499 **Figure 9.** TL glow curves of vermiculite irradiated with gamma rays at different doses.

500

501

502

503

504

505

506

507

508

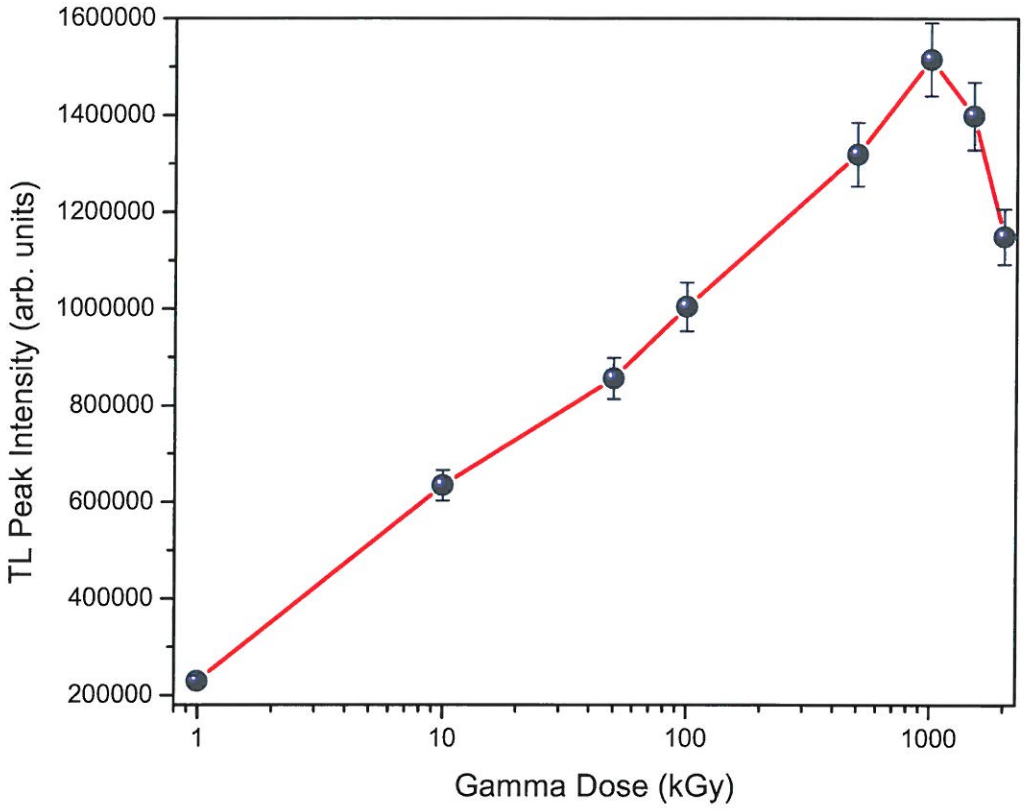

509

510 **Figure 10.** TL glow peak intensity vs gamma dose for vermiculite.

511

This is a preprint, the final version is subject to change, of the American Mineralogist (MSA)
Cite as Authors (Year) Title. American Mineralogist, in press.
(DOI will not work until issue is live.) DOI: http://dx.doi.org/10.2138/am-2014-4873 4/30

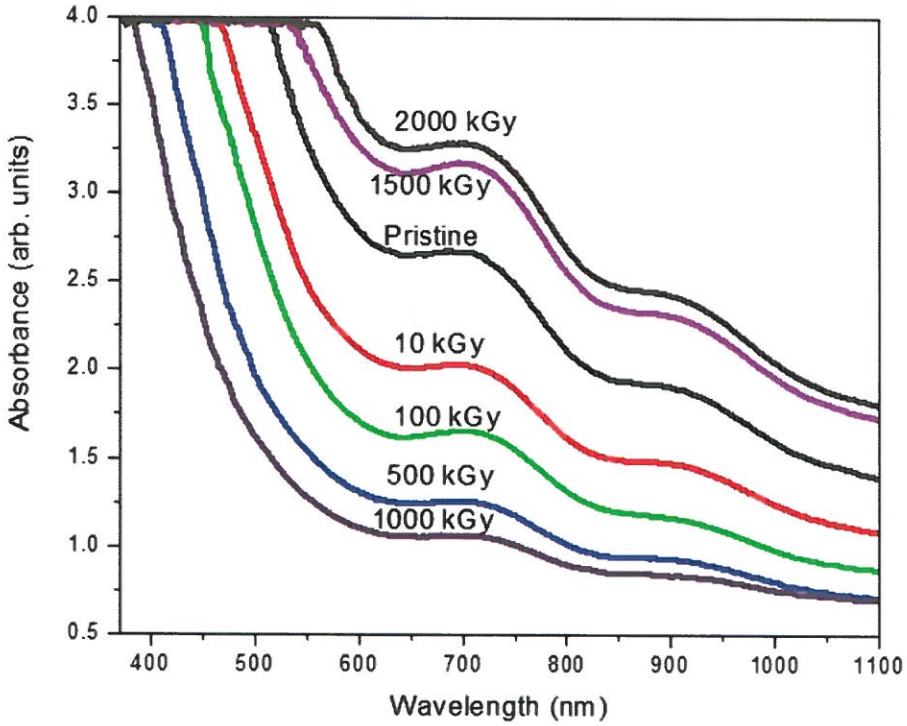

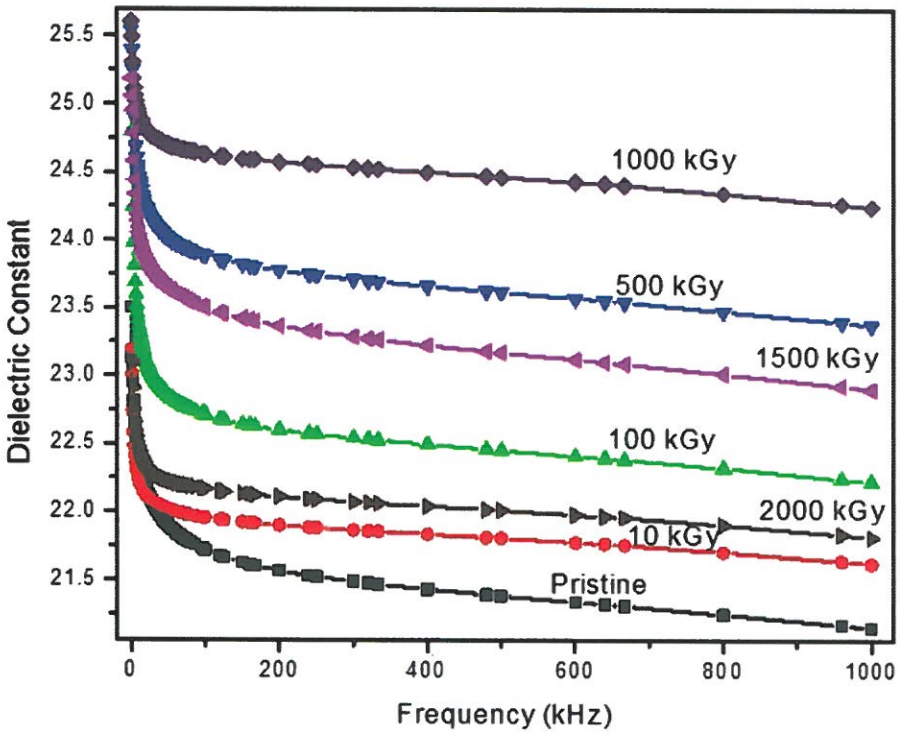

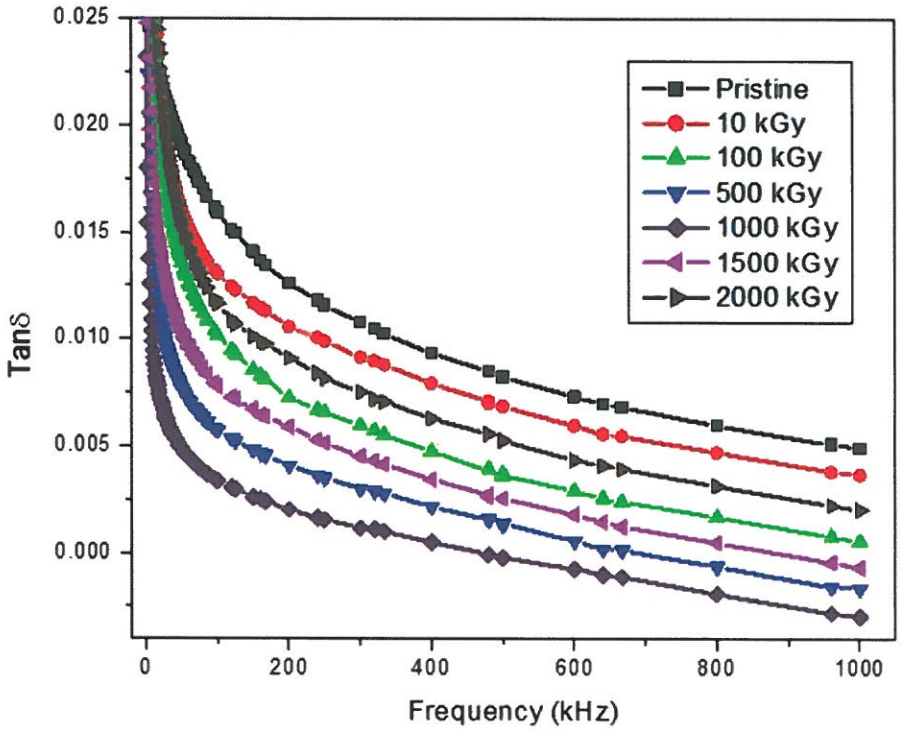

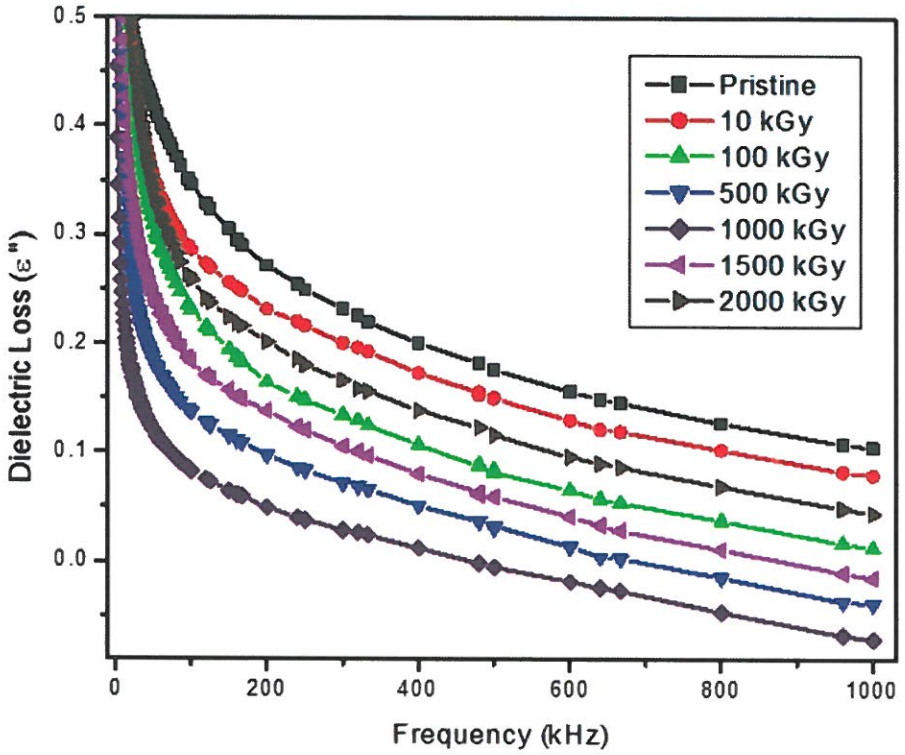

This is a preprint, the final version is subject to change, of the American Mineralogist (MSA)
Cite as Authors (Year) Title. American Mineralogist, in press.
(DOI will not work until issue is live.) DOI: http://dx.doi.org/10.2138/am-2014-4873 4/30

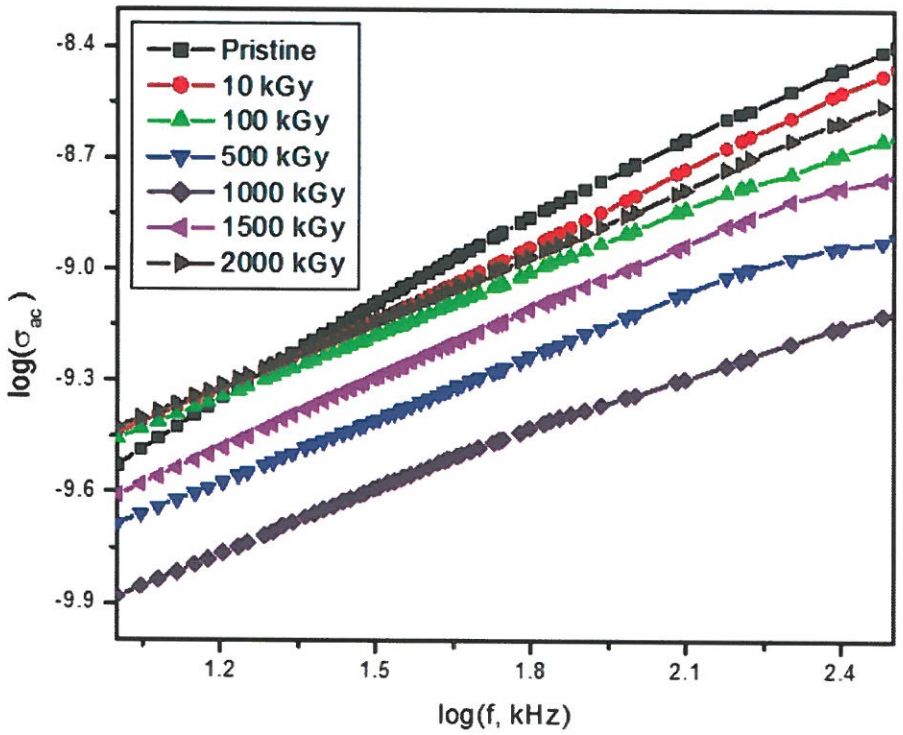

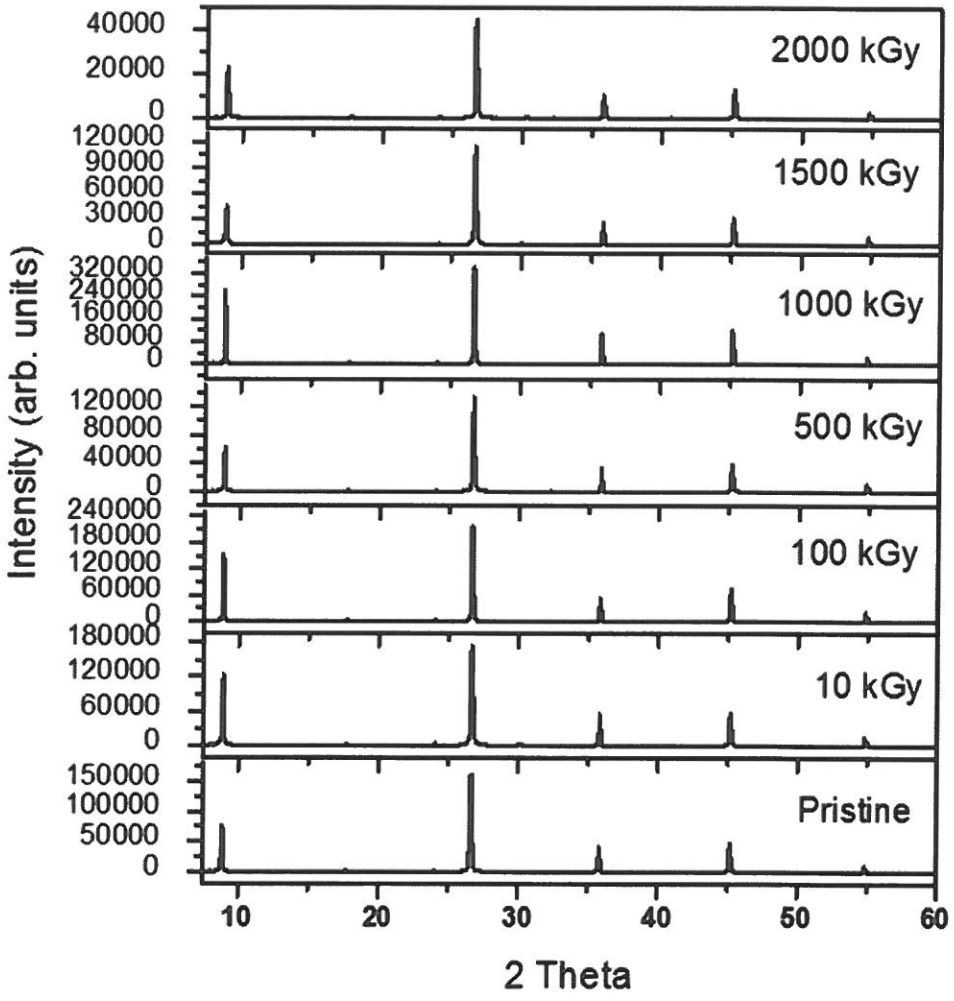

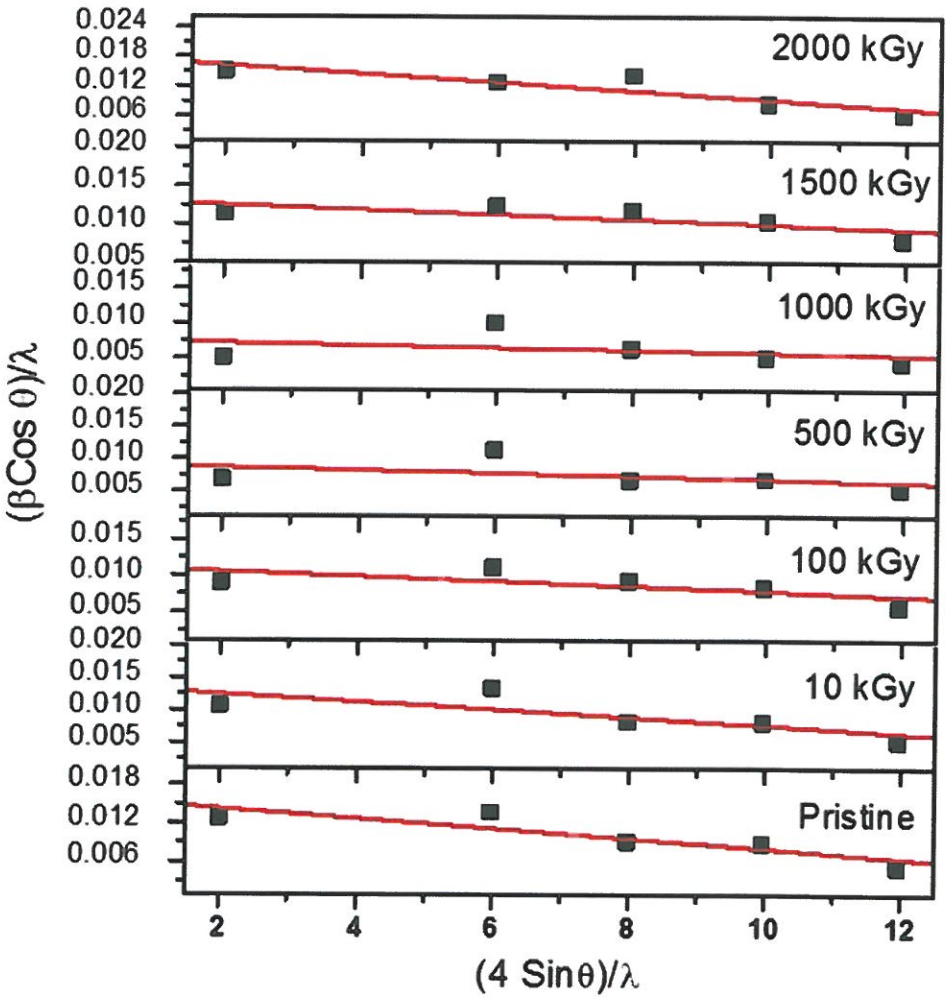

This is a preprint, the final version is subject to change, of the American Mineralogist (MSA)
Cite as Authors (Year) Title. American Mineralogist, in press.
(DOI will not work until issue is live.) DOI: http://dx.doi.org/10.2138/am-2014-4873 4/30